

SPIN-UP FROM REST OF A LIGHT-PARTICLE SUSPENSION IN A CYLINDER: THEORY AND OBSERVATIONS

M. UNGARISH

Department of Computer Science, Technion—Israel Institute of Technology, Haifa 32000, Israel

(Received 30 March 1990; in revised form 5 September)

Abstract—The spin-up from rest flow in a cylindrical container, filled with a homogeneous suspension of light particles in a fluid, and instantaneously set into rapid rotation around its axis of symmetry, is investigated. An asymptotic solution of the “mixture” averaged continuum equations is developed, which indicates that the velocity field is similar to that of a homogeneous fluid. However, a remarkable distribution of the particle volume fraction, $\varepsilon(r, z, t)$, governed by λ (= ratio of separation to spin-up time scales) shows up. A curved non-cylindrical interface is predicted to separate the shrinking mixture domain and the pure fluid accumulating near the cylindrical wall. Photographs taken in simple laboratory tests are presented, which qualitatively confirm the theoretical predictions on the shape and motion of the interface.

Key Words: rotating mixture/suspension, spin-up, centrifugal separation, interface, experiment, Ekman layers.

1. INTRODUCTION

Spin-up from rest of a fluid is a very common, yet quite complex phenomenon. Essentially, it concerns the transient motion performed by an initially stationary fluid which is subsequently exposed to the action of a spinning solid boundary and eventually acquires a steady-state of prevailing angular velocity (ideally, a state of “solid body rotation”). Spin-up from rest is, obviously, an intrinsic stage of centrifugal processing of suspensions. In this context it deserves special attention because: (a) a considerable separation may take place before the conventional $\Omega^* \times (\Omega^* \times \mathbf{r}^*)$ centrifugal field is established in the mixture; (b) an inverse stratification (i.e. heavier fluid at smaller radii) arises, which is a potential trigger of an instability, remixing convection; and (c) the prediction and analysis of the complicated, non-intuitive flow field and particle distribution is a stringent test for two-phase flow methodology.

A fundamental configuration for investigating spin-up is the cylindrical container, instantaneously set into rapid rotation, Ω^* , around its axis of symmetry. When the filling fluid is homogeneous, the governing parameters are the Ekman number, $E = \mu_c^*/\rho_c^* \Omega^* r_o^{*2}$; the aspect ratio, $H = H^*/r_o^*$ and the Froude number, $Fr = \Omega^* r_o^{*2}/g^*$. Here ρ_c^* and μ_c^* denote the density and viscosity of the fluid, respectively; Ω^* , r_o^* and H^* are the angular velocity, outer radius and height of the container, respectively; and g^* is the gravity acceleration (the asterisk designates dimensional variables). In rapid rotation $E \ll 1$, $Fr^{-1} \ll 1$. In this case, the classical solutions (Wedemeyer 1964; Greenspan 1968) elucidate the following leading features, see figure 1: an inwardly moving cylindrical “spin-up front” separates between the non-rotating inner core (I) and the partly spun-up region III; the quasi-steady Ekman layers (of thickness $\sqrt{\mu_c^*/\rho_c^* \Omega^*}$, on the top and bottom caps, referred to as region II) continuously extract fluid from sector I and feed it into domain III. The process is effectively completed when all the non-rotating fluid has been flushed into region III, and the typical spin-up time scale is $\tau_{su}^* = [(E^{1/2}/H)\Omega^*]^{-1}$. This simple “Wedemeyer model” has been subjected to refinements and verifications (Venezian 1970; Hyun *et al.* 1983) which shed more light on the flow field but are beyond the scope of the present discussion.

Consider again the above-mentioned cylinder, but now filled with a mixture of particles (or droplets) of radius a^* and density ρ_p^* in a continuous fluid. Initially, the stationary mixture is well-blended, therefore, the volume fraction of particles $\varepsilon(\mathbf{r}^*; t^* = 0) = \varepsilon(0) = \text{constant}$ throughout the cylinder. Again, the angular velocity Ω^* is imposed on the container at $t^* = 0$ and the subsequent flow field is of concern. As compared to Wedemeyer’s problem, three additional basic

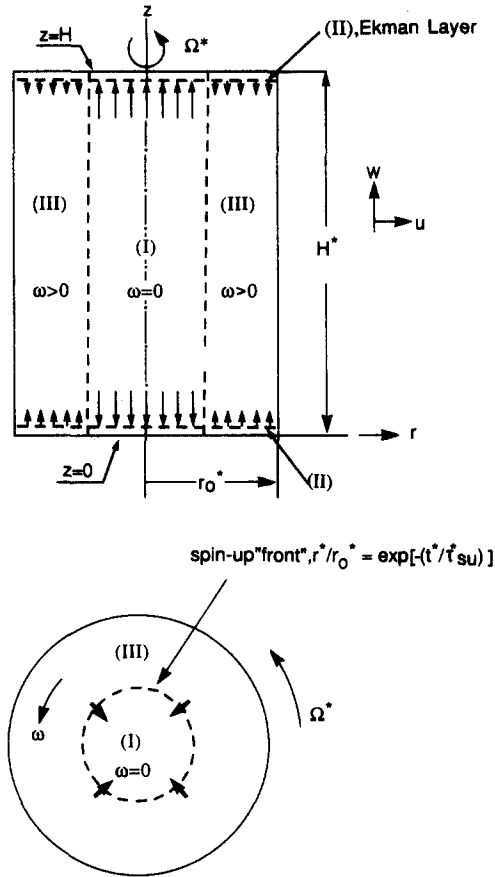


Figure 1. Basic features of spin-up flow in Wedemeyer's problem (homogeneous fluid).

dimensionless parameters show up: the density difference, $\alpha = (\rho_D^* - \rho_C^*)/\rho_C^*$; the (modified) particle Taylor number $\beta = \frac{2}{3} a^* \Omega^* \rho_C^* / \mu_C^*$; and the initial volume fraction $\varepsilon(0)$. From the physical standpoint, a new effect is introduced, namely, the separation of the suspension due to centrifugal buoyancy, associated with the time scale $\tau_{sep}^* = (|\alpha| \beta \Omega^*)^{-1}$. The analysis of the corresponding mixture spin-up problem has been attempted elsewhere (Ungarish 1990) for small E , α , β and $\varepsilon(0)$. In this pertinent range of parameters, the mixture velocity field is, to leading order, similar to that of a homogeneous fluid under identical spin-up circumstances, see figure 1. However, the evolution of this velocity field is accompanied by a very special change of the particle volume fraction, $\varepsilon(\mathbf{r}^*, t^*)$. In the non-rotating core (I) there is obviously no centrifugal buoyancy and $\varepsilon = \varepsilon(0)$. Mixture from this region is convected so rapidly through the Ekman layers that separation is insignificant and $\varepsilon = \varepsilon(0)$ also prevails in region II. On the other hand, the mixture entering region III is thereafter subjected to the centrifugal action of its own angular velocity and, while moving inward, undergoes separation. Since the angular velocity is dependent on both time and radius and unseparated mixture is continuously supplied near the endplates, the profile of $\varepsilon/\varepsilon(0)$ will be a non-trivial function of time, radius and axial distance from the endplates. The detailed distribution of particles is governed by two parameters: $\lambda (= E^{1/2}/|\alpha| \beta H)$, the ratio between separation and spin-up scales; and $s (= \alpha/|\alpha|)$, the sign of the buoyant force acting on the dispersed phase.

The previous study concentrated on the $s = 1$ case, corresponding to heavy particles, and the objective of the present paper is to investigate the $s = -1$ setting, for particles lighter than the embedding fluid. There is a notable difference between these cases: for $s = 1$ the separated dispersed phase forms a sediment layer, with $\varepsilon = \varepsilon_M$, on the outer wall (figure 2); whereas for $s = -1$ the inwardly moving light particles are expected to leave a region of pure fluid between the outer wall and the mixture zone (figure 3). From the point of view of unsophisticated experimentation with suspensions, the above-mentioned difference is censorious.

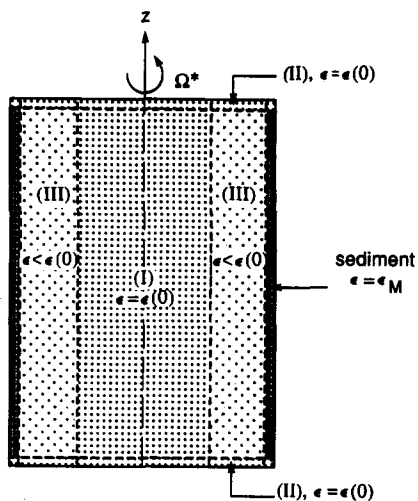


Figure 2. Qualitative, particle distribution during spin-up of a mixture of heavy particles ($s = 1$).

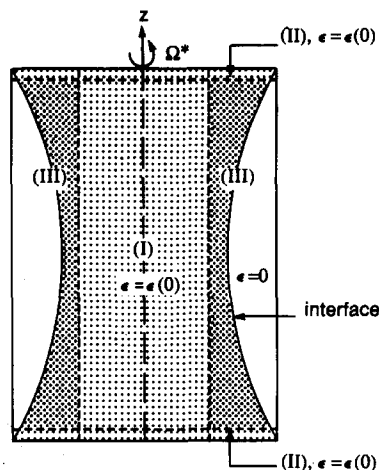


Figure 3. Qualitative, particle distribution during spin-up of a mixture of light particles ($s = -1$).

Common practice is to observe separation in a transparent container filled with a mixture of opaque particles in a transparent liquid. For spin-up, vision into the container through the endplates is obstructed by the particles, $\varepsilon = \varepsilon(0)$, in the Ekman layers that prevail on these walls. In the $s = 1$ case, the outer wall poses a similar obstacle, since it is covered by the sediment layer with $\varepsilon = \varepsilon_M$. On the other hand, in the $s = -1$ case the observation of the mixture through the outer wall of the cylinder is free. Moreover, for $s = -1$ theory predicts a peculiarly curved interface between the mixture and pure fluid domains whose shape and stability are worthy of scrutiny. Such an interface is a remarkable exception, since in conventional batch separation in simply shaped containers the geometry of the mixture–pure fluid interface is similar to that of the adjacent walls [a cylinder in the present case, see Greenspan (1983) and Ungarish & Greenspan (1984)].

Inspired by these considerations, this study focuses on the spin-up in a cylinder of a mixture of light particles. The theoretical background is presented in section 2 and some visualization tests are reported in section 3. The observed interface was essentially stable and its shape in fair agreement with theoretical expectations.

2. ANALYSIS

The averaged continuum “mixture” formulation (Ishii 1975) is employed. The mixture fluid is assumed Newtonian and its effective viscosity is incorporated via a semi-empirical correlation (Ishii & Zuber 1979):

$$\frac{\mu_{\text{eff}}^*}{\mu_C^*} = \mu(\varepsilon) = \left(1 - \frac{\varepsilon}{\varepsilon_M}\right)^{-2.5 \varepsilon_M}, \tag{1}$$

where ε_M is the maximal packing fraction.

The variables are scaled by the length r_o^* , density ρ_C^* , velocity $(\Omega^* r_o^*)$ and pressure $\rho_C^* (\Omega r_o^*)^2$. In view of [1], the effective Ekman number \mathcal{E} is related to the conventional parameters E by

$$\begin{aligned} \mathcal{E} &= ME, \\ M &= (\mu[\varepsilon(0)])^{1/2}; \end{aligned} \tag{2}$$

therefore, $[(\mathcal{E}^{1/2}/H)\Omega^*]^{-1}$ is the corresponding spin-up interval which scales the dimensionless time τ .

In an *inertial* frame of reference, the dimensionless equations of motion are:

total volume continuity,

$$\nabla \cdot \mathbf{j} = 0; \quad [3]$$

dispersed phase continuity,

$$\frac{\mathcal{E}^{1/2}}{H} \frac{\partial \varepsilon}{\partial \tau} + \nabla \cdot \mathbf{j}_D = 0; \quad [4]$$

and

momentum balance,

$$(1 + \alpha \varepsilon) \left(\frac{\mathcal{E}^{1/2}}{H} \frac{\partial \mathbf{v}}{\partial \tau} + \mathbf{v} \cdot \nabla \mathbf{v} \right) = -\nabla p + \mathcal{E} \nabla \cdot \{ \mu(\varepsilon) [\nabla \mathbf{v} + (\nabla \mathbf{v})^T - \frac{2}{3} \nabla \cdot \mathbf{v}] \} \\ - \nabla \cdot \varepsilon (1 - \varepsilon) \frac{1 + \alpha}{1 + \alpha \varepsilon} \mathbf{v}_R \mathbf{v}_R. \quad [5]$$

The basic kinematic relationships for mass velocities \mathbf{v} and volume fluxes \mathbf{j} read:

$$\mathbf{v}_R = \mathbf{v}_D - \mathbf{v}_C; \quad \mathbf{v} = \frac{[(1 + \alpha)\varepsilon \mathbf{v}_D + (1 - \varepsilon)\mathbf{v}_C]}{(1 + \alpha \varepsilon)}; \\ \mathbf{j}_D = \varepsilon \mathbf{v}_D; \quad \mathbf{j}_C = (1 - \varepsilon)\mathbf{v}_C; \quad \mathbf{j} = \mathbf{j}_D + \mathbf{j}_C; \quad [6a]$$

the subscripts C and D designate the continuous and dispersed phases, respectively. If ε and two of the velocities are known, the others can be calculated in a straightforward manner. In particular, one obtains

$$\mathbf{j}_D = \varepsilon \mathbf{j} + \varepsilon (1 - \varepsilon) \mathbf{v}_R; \quad \mathbf{j} = \mathbf{v} - \alpha \frac{\varepsilon (1 - \varepsilon)}{1 + \alpha \varepsilon} \mathbf{v}_R. \quad [6b]$$

The mixture model, which solves for \mathbf{v} and ε , requires a closure formula for the relative velocity, \mathbf{v}_R . It is assumed that the non-colloidal dispersed particles are very small ($\beta \ll 1$) the density difference is moderate ($|\alpha| < 1$) and the relative motion is slow ($\text{Re}_R = |\mathbf{v}_R^*| a^* \rho_C^* / \mu_C^* < 1$). In this case, the presumably dominant quasi-steady balance between the local ‘‘centrifugal buoyancy’’ and Stokesian drag yields

$$\mathbf{v}_R = -s \frac{1 - \varepsilon}{\mu(\varepsilon)} [\mathbf{v} \cdot \nabla \mathbf{v}] |\alpha| \beta. \quad [7]$$

This is not a centrifugal effect in the usual sense because an inertial frame of reference is used here. The ‘‘buoyant’’ acceleration of the particle is rather a dynamic result of the complicated, non-hydrostatic motion of the fluid. The contrast with the classical gravity sedimentation problems, for which solutions can be derived from kinematic continuity arguments (Kynch 1952; Davis & Russell 1989) is evident.

Initially, the mixture is motionless and homogeneously blended, $\mathbf{v} = 0$, $\varepsilon = \varepsilon(0)$, throughout the container. For $\tau \geq 0+$, the no slip—relative to the rotating walls—and no penetration boundary conditions are prescribed.

The physico-mathematical formulation is complete, but the analysis requires major simplifications. The investigation is subsequently restricted to the range of small $\mathcal{E}^{1/2}$, β , α and $\varepsilon(0)$, and moderate H , for which perturbation methods can be applied in the same manner as for the $s = 1$ case (Ungarish 1990). For the sake of completeness, some basic results are briefly rederived here. The cylindrical (r, θ, z) coordinates are used, where z is the axis of symmetry and $\mathbf{v} = u\hat{r} + v\hat{\theta} + w\hat{z}$. The dimensionless angular velocity of the container is $1\hat{z}$.

It can be argued that, in the above-mentioned range of parameters, the driving mechanism of the spin-up phenomena is the influx-efflux (‘‘suction’’) of the Ekman layers, which gives rise to axial velocities $O(\mathcal{E}^{1/2})$. An order of magnitude consideration indicates that outside these thin Ekman layers an inviscid interior prevails, whose dependent variables can be expanded in powers of $\mathcal{E}^{1/2}$

as follows:

$$\begin{aligned}
 u &= \frac{\mathcal{E}^{1/2}}{H} u_1(r, z, \tau) + \cdots; \\
 u_R &= \frac{\mathcal{E}^{1/2}}{H} u_{R1}(r, z, \tau) + \cdots; \\
 v &= r\omega_0(r, z, \tau) + \cdots; \\
 v_R &= \mathcal{E}^{1/2} v_{R1}(r, z, \tau) + \cdots; \\
 w &= \mathcal{E}^{1/2} w_1(r, z, \tau) + \cdots; \\
 w_R &= \mathcal{E} w_{R2} + \cdots; \\
 p &= p_0(r, z, \tau) + \cdots; \\
 \varepsilon &= \varepsilon(r, z, \tau) + \cdots.
 \end{aligned} \tag{8}$$

The subscript “0” of ε is deliberately omitted, to avoid confusion with $\varepsilon(0)$; in the subsequent analysis, ε refers to the leading term only. In addition it is assumed that $|\alpha|\varepsilon = O(\mathcal{E}^{1/2})$.

The velocity field

The radial, axial and azimuthal momentum equations yield, for the leading terms,

$$\omega_0^2 r = \frac{dp_0}{dr}; \tag{9}$$

and

$$\frac{\partial \omega_0}{\partial \tau} + u_1 \frac{1}{r^2} \frac{\partial}{\partial r} r^2 \omega_0 = 0. \tag{10}$$

Further substitution into the kinematic relationships [6b], gives, to leading order,

$$\mathbf{j} \cdot \hat{r} = \frac{\mathcal{E}^{1/2}}{H} u_1(r, \tau); \quad \mathbf{j} \cdot \hat{z} = \mathcal{E}^{1/2} w_1. \tag{11}$$

The volume continuity in a cylinder of radius r , from the bottom to top plates, can therefore be expressed as

$$2\pi r \mathcal{E}^{1/2} u_1(r, \tau) + 2\tilde{Q} = 0. \tag{12}$$

Here \tilde{Q} is the volume flux in one Ekman layer, which will be approximated by

$$\tilde{Q} = \pi \mathcal{E}^{1/2} r^2 (1 - \omega_0). \tag{13}$$

This formula for the Ekman layer transport, introduced by Wedemeyer (1964) (who actually used a slightly different coefficient of proportionality) is the result of a momentum-integral analysis. For homogeneous fluids, its validity can be proven in the limit $\omega_0 \rightarrow 1$ and there is a great deal of evidence that it reproduces the main features of the Ekman layer “suction” in quite general flows. The applicability of this correlation to mixtures can be heuristically justified if β , α and ε are small; additional support in this direction has been provided by numerical results (Ungarish 1988).

Equations [9]–[13], with the appropriate boundary conditions, constitute the classical inviscid model for spin-up. Thus, to leading order, the velocity field of the spun-up mixture is identical with that of a homogeneous fluid, as summarized in table 1.

For the relative velocity, [7] and [8] yield

$$\frac{\mathcal{E}^{1/2}}{H} u_{R1} = s |\alpha| \beta \frac{(1 - \varepsilon)}{\mu(\varepsilon)} \omega_0^2 r \tag{14}$$

or, in a more convenient form,

$$u_{R1} = s \frac{1 - \varepsilon}{\lambda M} \frac{1}{\mu(\varepsilon)} \omega_0^2 r, \tag{15}$$

Table 1. Velocity field outside the Ekman layers; here
 $A = A(\tau) = e^{-2\tau}$

	Region I, $0 \leq r^2 \leq A$	Region III, $A \leq r^2 \leq 1$
u_1	$-r$	$\frac{A}{1-A} \left(r - \frac{1}{r} \right)$
ω_0	0	$\frac{1}{1-A} \left(1 - \frac{A}{r^2} \right)$
w_1	$\left(2 \frac{z}{H} - 1 \right)$	$-\frac{A}{1-A} \left(2 \frac{z}{H} - 1 \right)$

where, again,

$$\lambda = \frac{E^{1/2}}{|\alpha| \beta H}. \quad [16]$$

The evaluation of v_{R1} and w_{R2} is omitted because it can be shown that they do not contribute leading order terms to the distribution of the dispersed phase, the next object of investigation.

The volume fraction and the mixture-pure fluid interface

Equation [15] and table 1 indicate that a significant interphase radial motion takes place in region III and a redistribution of the volume fraction, ε , is expected. A convenient equation for this variable is obtained by combining [4], [3] and [6b] into

$$\frac{\mathcal{E}^{1/2}}{H} \frac{\partial \varepsilon}{\partial \tau} + \mathbf{j} \cdot \nabla \varepsilon + \nabla \cdot \varepsilon (1 - \varepsilon) \mathbf{v}_R = 0. \quad [17]$$

The corresponding balance for the leading terms of the expansion [8] yields, after arrangement,

$$\frac{\partial \varepsilon}{\partial \tau} + \left[u_1 + s \frac{1}{\lambda M} \Phi'(\varepsilon) \omega_0^2 r \right] \frac{\partial \varepsilon}{\partial r} + w_1 H \frac{\partial \varepsilon}{\partial z} = -s \frac{1}{\lambda M} \Phi(\varepsilon) \frac{1}{r} \frac{\partial}{\partial r} \omega_0^2 r^2, \quad [18]$$

where

$$\Phi(\varepsilon) = \frac{\varepsilon(1-\varepsilon)^2}{\mu(\varepsilon)}$$

and ω_0 , u_1 and w_1 are explicitly defined in table 1. The initial condition is $\varepsilon(\mathbf{r}, 0) = \varepsilon(0)$. For the solution of [18], three regions should be distinguished:

- Region I: the non-rotating interior, $0 \leq r \leq e^{-\tau}$. Since $\omega_0 = 0$, the solution of [18] is simply $\varepsilon = \varepsilon(0)$ throughout this region.
- Region II: the Ekman layers. According to table 1, these layers absorb mixture from region I, where $\varepsilon = \varepsilon(0)$. Any element of the absorbed fluid is transported to larger radii and effluxed into region III. The time elapsed between the influx and efflux of the element is $O(\Omega^{*-1})$, much smaller than the separation interval, $O[|\alpha| \beta \Omega^{*-1}]$. Consequently, fluid in the Ekman layers can be regarded as an extension of the mixture in region I, with $\varepsilon = \varepsilon(0)$.
- Region III: the rotating interior, $e^{-\tau} \leq r \leq 1$. Here considerable departure from $\varepsilon(0)$ is expected, because: (a) the r.h.s. of equation [18] is $O(-s/\lambda)$; and (b) when $s = -1$, a large domain of pure fluid, $\varepsilon = 0$, develops, and when $s = 1$ a sediment layer, $\varepsilon = \varepsilon_M$, appears. The boundary condition for the solution is derived from the important observation that region III contains only fluid effluxed by the Ekman layers (region II). Recalling the properties of region II, the boundary conditions become:

$$\varepsilon = \varepsilon(0) \quad \text{at } z = 0, H \quad (e^{-\tau} \leq r \leq 1).$$

The value of $\varepsilon(r, z, \tau)$ in the mixture domain of region III can now be calculated by the method of characteristics. Due to symmetry, only $0 \leq z \leq H/2$ needs consideration. Upon using the notation,

$$x = r^2, \quad A = A(\tau) = e^{-2\tau}, \quad [19]$$

the characteristic equivalent of [18] is

$$\frac{d\varepsilon}{d\tau} = -s \frac{2}{\lambda M} \Phi(\varepsilon) \left[\frac{1 - A^2}{(1 - A)^2} \right], \quad [20a]$$

on the path

$$\frac{dx}{d\tau} = 2 \frac{A}{1 - A} x \left[1 - \frac{1}{x} + s \frac{1}{\lambda M A(1 - A)} \frac{\Phi'(\varepsilon)}{\Phi(\varepsilon)} \left(1 - \frac{A}{x} \right)^2 \right], \quad [20b]$$

$$\frac{dz}{d\tau} = \frac{A}{1 - A} \left(1 - 2 \frac{z}{H} \right) H, \quad [20c]$$

subject to

$$\varepsilon = \varepsilon(0) \quad \text{on } z = 0, \quad A \leq x \leq 1. \quad [21]$$

If the term in brackets in [20a] equals 1, the conventional solid-body ($\omega_0 = 1$) rate of separation is recovered.

The axial characteristic trajectory is unaffected by buoyancy and [20c] can be readily integrated:

$$\frac{z}{H} = \frac{1}{2} \left[1 - \frac{1 - e^{-2\tau_{in}}}{1 - A} \right]. \quad [22]$$

This means that all the mixture particles in region III whose axial position is (z/H) at instance τ , have been effluxed by the Ekman layers at τ_{in} in the sector $e^{-2\tau_{in}} \leq r^2 \leq 1$. In particular, the locus $e^{-2\tau} \leq r^2 \leq 1$, (z/H) = 1/2, at instance τ corresponds to characteristics emitted from the corner $\tau_{in} = 0$, $r = 1$, $z = 0$. Since in this corner the inviscid solution displays a non-physical behaviour, the resulting characteristics are not reliable and, therefore, have been excluded from the present approximation. It can be argued that viscous diffusion and relaxation delay will eliminate that singularity in which case a smooth ε , with $(\partial\varepsilon/\partial z) = 0$ at $z = H/2$, is expected.

The cases $s = -1$ (light particles) is subsequently treated in detail. It is evident from [20a] that $\varepsilon(r, z, \tau)/\varepsilon(0) \geq 1$ throughout the mixture region. Global volume conservation of the dispersed phase therefore requires that the volume occupied by the mixture shrinks, i.e. an expanding domain of pure fluid, $\varepsilon = 0$, shows up. To explore this conclusion, consider the trajectory (x_D, z_D) of a dispersed particle, effluxed into domain III at $z = 0$, $\tau = \tau_{in}$ and $x = x_{in}$ ($A \leq x_{in} \leq 1$). Employing the kinematic relation $\mathbf{v}_D = \mathbf{v} + (1 - \varepsilon)\mathbf{v}_R/(1 + \alpha\varepsilon)$, [15] and table 1, it follows that, to leading order, the radial component satisfies

$$\frac{dx_D}{d\tau} = 2 \frac{A}{1 - A} x \left[1 - \frac{1}{x} - \frac{1}{\lambda M A(1 - A)} \frac{\Phi(\varepsilon)}{\varepsilon} \left(1 - \frac{A}{x} \right)^2 \right], \quad [23]$$

and z_D is given by [22]. Since the r.h.s of [23] is negative, x_D is a monotonically decreasing function of τ (or z_D); thus, the particles always move toward the axis of rotation, as expected. In particular, the locus of particles effluxed at $x_{in} = 1$, $\tau_{in} \leq \tau$ demarcates the domain beyond which no particles can be found at instance τ . The typical shape is depicted in figure 3. This is a kinematic shock, the interface between mixture and pure fluid domains. It can be shown that this shock is "stable" from the point of view of the characteristics [20b, c].

In general, [19]–[23] should be solved numerically, for given parameters λ , H , $\varepsilon(0)$ and ε_M . Some simplification in calculation and representation is gained in the dilute limit, $\varepsilon \rightarrow 0$, where $\Phi(\varepsilon) = \varepsilon$, $\mu(\varepsilon) = 1$ and $M = 1$. In this case, the kinematic shock [23] coincides with the outmost characteristic [20b] emanated at $x = 1$. The representative solutions, figures 4 and 5, indicate that the parameter

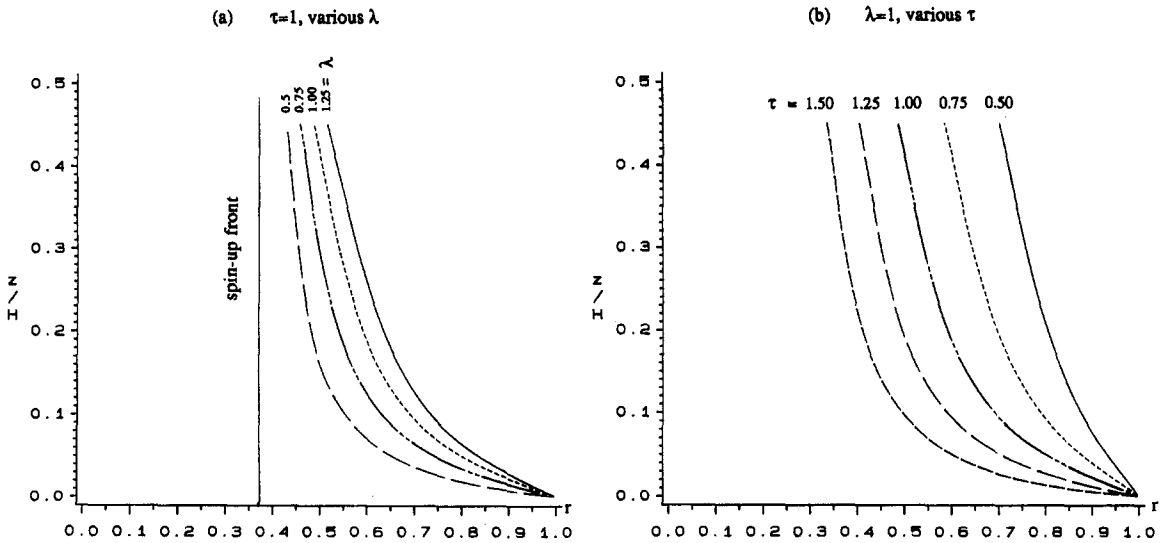


Figure 4. Motion of the interface (theory, dilute case): (a) $\tau = 1$, various λ ; (b) $\lambda = 1$, various τ .

λ has a strong influence on both $\varepsilon/\varepsilon(0)$ and the motion of the shock. In general, $\varepsilon/\varepsilon(0)$ increases with time, radial distance from the spin-up front, $r - e^{-\tau}$, and axial distance from the endplate (Ekman layer). As λ decreases, the central part of the shock moves faster and its “heap” near the endplate is thinner.

The trends of the present solution for large λ are of special interest. In this limit (see the appendix) the locus of the interface (or outmost characteristic) is approximated by

$$x_D(\tau, z) = 1 - \frac{1}{\lambda} (1 - A) \ln \frac{1 - (1 - A)Z}{AZ} + O\left(\frac{1}{\lambda^2}\right) \tag{24}$$

and the corresponding volume fraction satisfies

$$\ln[\varepsilon(\tau, z)/\varepsilon(0)] = \frac{1}{\lambda} \ln \frac{1 - (1 - A)Z}{AZ^2} + O\left(\frac{1}{\lambda^2}\right), \tag{25}$$

where $Z = (1 - 2z/H)$ and $A = e^{-2\tau}$. This indicates that when λ is large, the spin-up stage $\tau \leq 2$ has a minor influence on the distribution of the particles. In this case, the more conventional concept of centrifugal separation can be applied, i.e. the process can be regarded as starting with a mixture in solid body rotation and $\varepsilon = \varepsilon(0)$, throughout the cylinder.

It is important to notice that for $\lambda \leq 1$ the ratio $\varepsilon/\varepsilon(0)$ attains large values during spin-up. The dilute approximation is therefore valid only in the initial stages, unless $\varepsilon(0)$ is indeed very small. In the non-dilute case, the shock intersects characteristics and the integration of [23] is coupled to the solution of [20]–[22] via the value of ε on the shock. Actually, this calculation requires interpolations in x only by taking advantage of the fact that [22] applies to both particles and characteristics. The non-diluteness hinders the motion of the interface and the growth of ε .

It is recalled that $\rho = 1 + \alpha\varepsilon$, therefore, in the present $\alpha < 0$ case, an increase of ε means a decrease of the mixture density. The results in figure 5 and table 1 clearly indicate an inverse radial stratification in the mixture region, i.e. the density is maximal in the non-rotating domain I, but in domain III it continuously decreases with r , while ω increases. The stability of this structure is questionable, but the analytical treatment of this topic was not pursued here. This issue received attention during the experimental tests, and the conjecture is that the stable solution is practically valid for small α and $\varepsilon(0)$.

3. LABORATORY TEST

Simple qualitative experiments have been performed to test the theoretical predictions concerning the shape and motion of the interface. In addition, some indication on the stability of the flow was

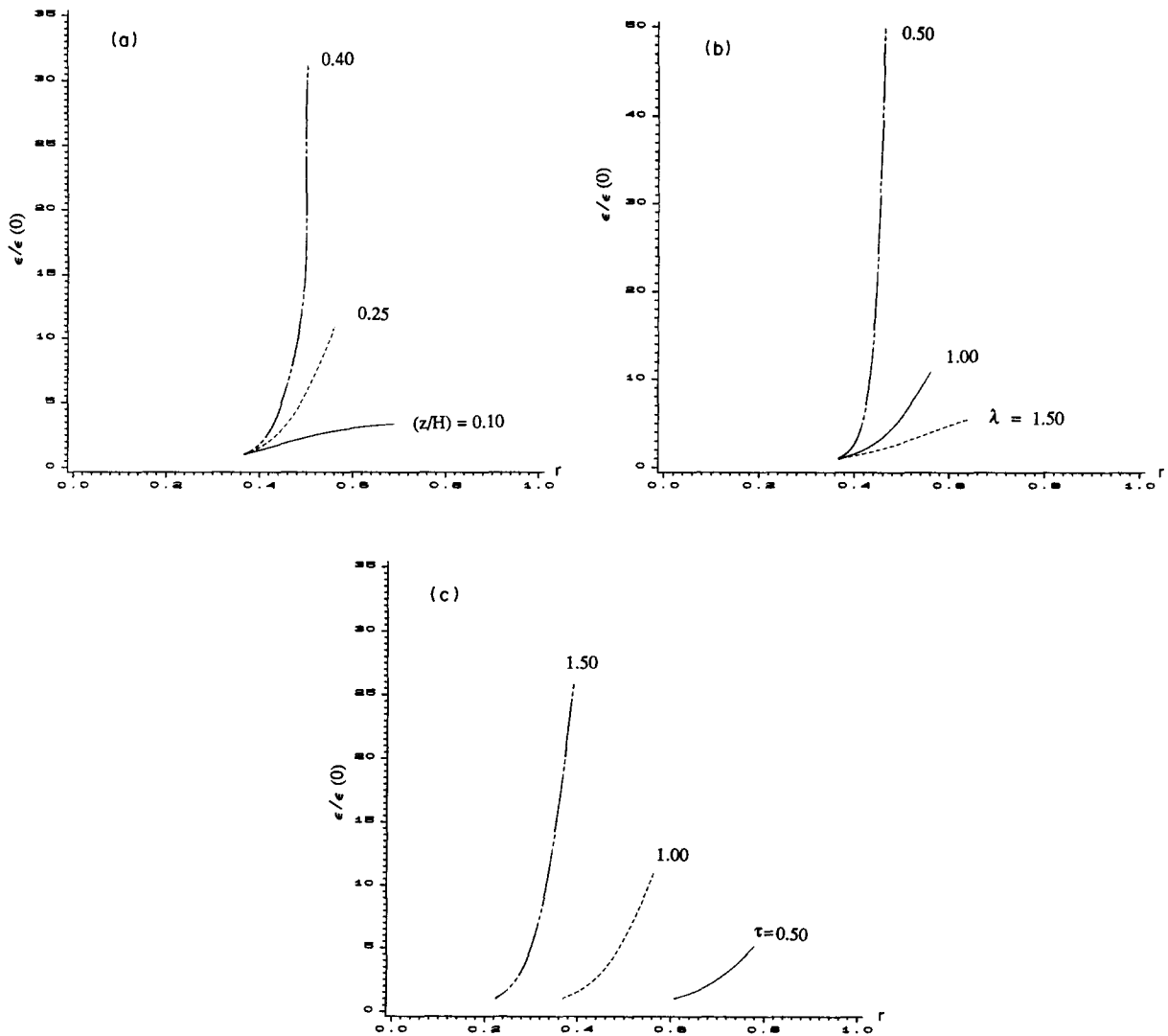


Figure 5. Volume fraction, $\epsilon/\epsilon(0)$, vs r (theory, dilute case): (a) $\lambda = 1.0$, $\tau = 1.0$, various (z/H) ; (b) $(z/H) = 0.25$, $\tau = 1.0$, various λ ; (c) $(z/H) = 0.25$, $\lambda = 1.0$, various τ .

sought. For observation and record purposes, the basic requirements were a spin-up interval of at least 20 s while $0.5 < \lambda < 1.5$, which impose some compromises on other desired parameters.

A cylindrical transparent container ($r_0^* = 9.55$ cm, $H^* = 20.0$ cm) placed on a turntable was used. The transparent continuous phase contains one-third glycerine and two-thirds water and the dispersed phase consists of opaque (white) polystyrene beads, sieved in the range $3.00 \cdot 10^{-2} < 2a^* < 3.55 \cdot 10^{-2}$ cm. The representative properties are: $\epsilon(0) = 0.01$, $\rho_c^* = 1.082$ g/cm³, $\mu_c^*/\rho_c^* = 0.029$ cm²/s, $\alpha = -0.034$ and $a^* = 1.64 \cdot 10^{-2}$ cm. The tested angular velocities and the resulting parameters are listed in table 2. The thickness of the Ekman layers in these tests is around 0.5 mm.

Table 2

$\Omega^*(\text{rpm})$	λ	$E^{1/2}(\cdot 10^{-3})$	$\beta(\cdot 10^{-2})$	$\tau_{\text{sep}}^*(\text{s})$	$\tau_{\text{su}}^*(\text{s})$	Re_{Rmax}	Fr
200	1.26	3.89	4.32	32.26	25.65	0.17	4.29
250	0.90	3.48	5.40	20.65	22.94	0.26	6.70
300	0.68	3.18	6.48	14.34	20.94	0.38	9.64
350	0.54	2.94	7.56	10.53	19.39	0.51	13.13

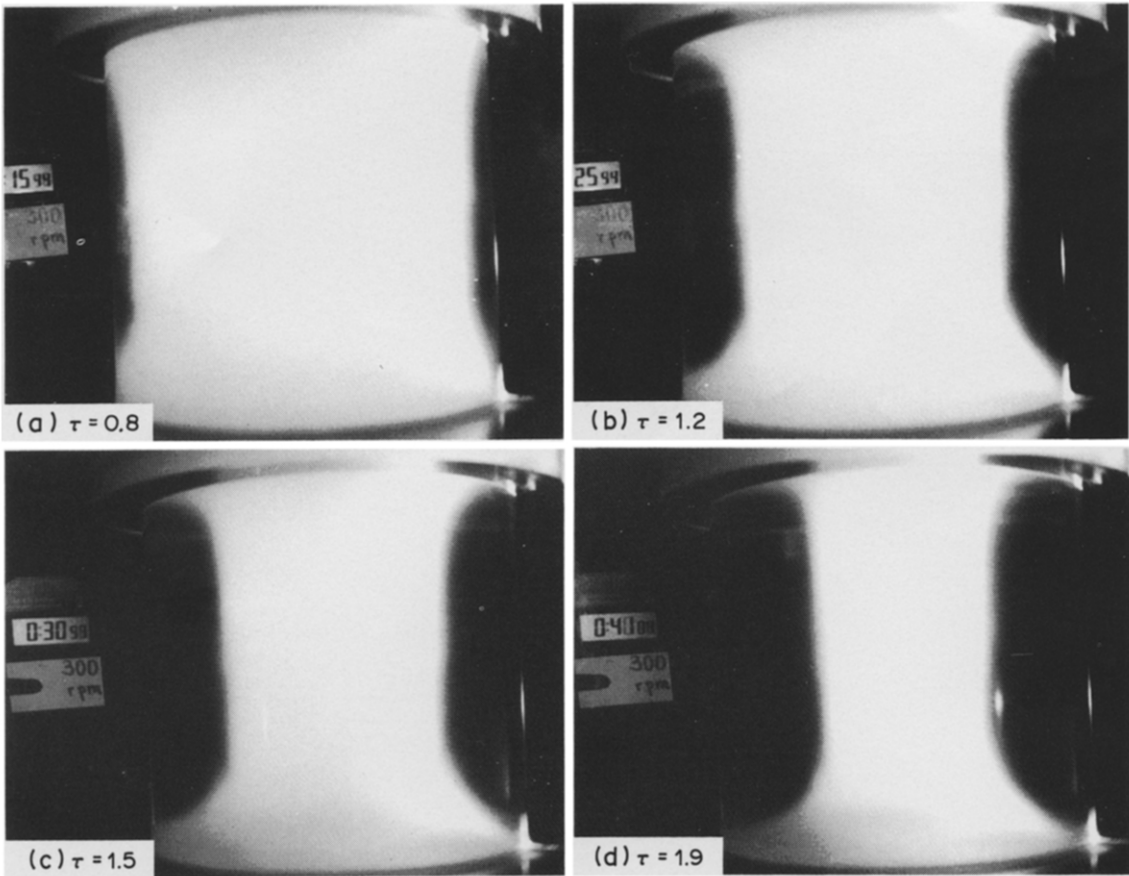


Figure 6(a)–(d). *Legend opposite.*

The tests were as follows. Initially, the suspension was mixed by randomly shaking and tumbling the container, and then placed on the stationary turntable. After a short rest, the motor was switched on to the preset angular velocity. The subsequent motion in the cylinder was scrutinized under a slit beam in the (r, z) plane, and pictures were taken with a rapid Polaroid camera.

All the tested cases were in essential agreement with the theoretical predictions: two distinct domains, of mixture and pure fluid, have been observed. The interface between these domains was a bit blurred, but certainly of curved, non-cylindrical, form—and attached to the rims $(r = 1, z = 0, z = H)$ of the cylinder during at least $2\tau_{su}^*$. The blurs of the interface can be attributed to non-uniformities in particle size and shape, local smoothing motions (not captured by the first-order theory) and the slow onset of instabilities. However, no clear-cut indication of flow instability was observed on the interface, interior or boundary layers.

Some photographs, accompanied by the corresponding theoretical shape of the interface, are presented here. (The container has an outer ring which covers 1.8 cm of the upper part, therefore the symmetry with respect to the midplane is not apparent in the photographs.) Figure 6 shows the position of the interface for $\lambda = 0.68$, at different τ . The interface is practically attached to the rims of the circular endplates during $\tau \leq 1.9$. At $\tau = 2.7$, however, for $r \geq 0.75$, ω is so close to 1 that the Ekman layer suction in this region is too weak to drag the particles to the periphery, against the buoyancy force. The qualitative agreement between the predicted and observed motion is good.

Figure 7 shows the position of the interface for two different systems, $\lambda = 1.26$ and 0.54 , at approximately the same τ . For the smaller λ , the center of the interface moved farther from the outer wall and the heap on the endplate is thinner. Again, the qualitative agreement with the theory is good.

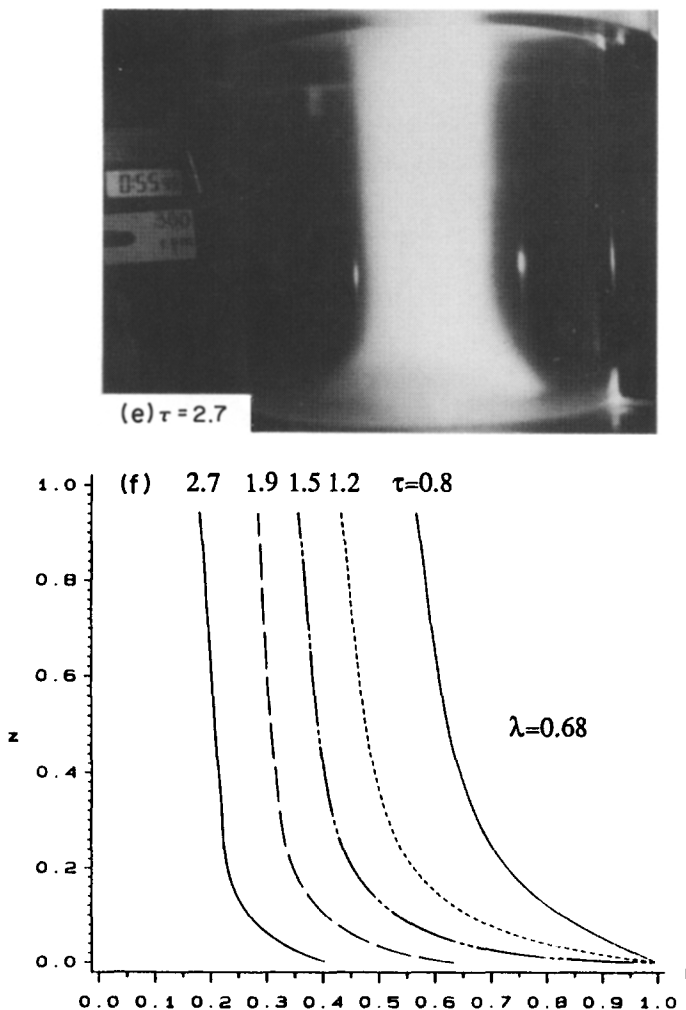


Figure 6. (a)–(e) Test, $\lambda = 0.68$, $\tau = 0.8, 1.2, 1.5, 1.9$ and 2.7 ; (f) calculated interfaces [$\varepsilon(0) = 0.01$, $\varepsilon_M = 0.65$].

4. CONCLUDING REMARKS

The spin-up from rest in a cylinder, filled with a mixture of light particles and fluid, has been considered. The asymptotic analysis of the averaged continuum mixture model—for small E , α , β , $\varepsilon(0)$ and $H = O(1)$ —predicts a peculiar space–time variation of the particle volume fraction, ε , governed mainly by the parameter $\lambda (= E^{1/2}/|\alpha|\beta H)$. When $\lambda \leq 1$, significant separation accompanies the spin-up process: large values of $\varepsilon/\varepsilon(0)$ show up in the mixture domain and a growing region of pure fluid forms adjacent to the outer wall. The expected shape of the moving mixture–pure fluid interface is remarkably different from that of the boundaries.

The simple laboratory tests reported here confirm, qualitatively, the theoretical results concerning the shape and motion of the interface. The visualized flow fields were apparently stable.

These results illuminate new physical aspects of the mixture separation process. Also, they provide additional confidence in the predictive power of the “averaged continuum” models—for which very few verified non-trivial solutions are presently available.

Sophisticated experiments are still required for a more comprehensive confirmation of the theory, especially regarding the values of ε . Further analytical efforts are necessary for understanding viscous effects and the stability restrictions of the investigated flow field.

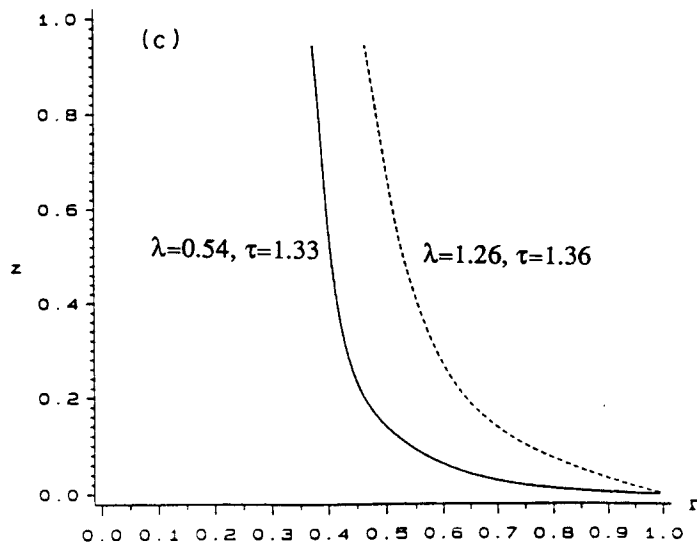
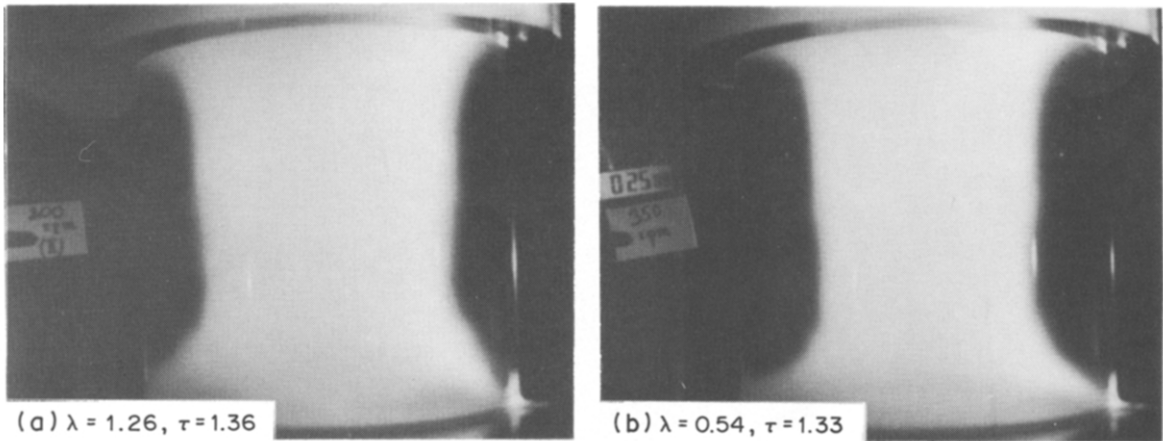


Figure 7. (a) Test, $\lambda = 1.26$, $\tau = 1.36$; (b) test, $\lambda = 0.54$, $\tau = 1.33$; (c) calculated interfaces [$\varepsilon(0) = 0.01$, $\varepsilon_M = 0.65$].

Acknowledgements—The experiments were performed at the Fluid Dynamics Laboratory, Applied Mathematics, MIT, Cambridge, Mass., with the help of Professor HP Greenspan and Dr A A Dahlkild. This research was partially supported by the NSF, Grant 8519764-DMS. The paper was written during a visit to the Department of Computer Science, University of the Witwatersrand.

REFERENCES

- DAVIS, K. W. & RUSSELL, W. B. 1989 An asymptotic description of transient settling and ultrafiltration of colloidal dispersions. *Phys. Fluids* **A1**, 82–100.
- GREENSPAN, H. P. 1968 *The Theory of Rotating Fluids*, Sect. 3.7. Cambridge Univ. Press, Cambs.
- GREENSPAN, H. P. 1983 On centrifugal separation of a mixture. *J. Fluid Mech.* **127**, 91–101.
- HYUN, J. M., LESLIE, F., FOWLIS, W. W. & WARN-VARNAS, A. 1983 Numerical solutions for spin-up from rest in a cylinder. *J. Fluid Mech.* **127**, 263–281.
- ISHII, M. 1975 *Thermo-fluid Dynamic Theory of Two-phase Fluid*. Eyrolles, Paris.
- ISHII, M. & ZUBER, N. 1979 Drag coefficient and relative velocity in bubbly, droplet or particle flows. *AIChE JI* **25**, 843–854.
- KYNCH, G. J. 1952 A theory of sedimentation. *Trans. Faraday Soc.* **48**, 166–176.
- UNGARISH, M. 1988 Numerical investigation of two-phase rotating flow. *Int. J. Multiphase Flow* **14**, 729–747.
- UNGARISH, M. 1990 Spin-up from rest of a mixture. *Phys. Fluids* **A2**, 160–166.

UNGARISH, M. & GREENSPAN, H. P. 1984 On centrifugal separation of particles of two different sizes. *Int. J. Multiphase Flow* **10**, 133–148.

VENEZIAN, G. 1970 Nonlinear spin-up. *Top. Ocean Engng* **2**, 87–96.

WEDEMEYER, E. H. 1964 The unsteady flow within a spinning cylinder. *J. Fluid Mech.* **20**, 383–399.

APPENDIX

Introduce the transformed variables:

$$T = 1 - A; \quad \xi = 1 - x; \quad Z = 1 - 2 \frac{z}{H};$$

(recall, $A = e^{-2\tau}$). Equation [22] now reads

$$TZ = T_{in}. \quad [\text{A.1}]$$

For the dilute case, [20a, b] yield:

$$\frac{d\varepsilon}{dT} = \varepsilon \frac{1}{\lambda} \frac{1}{(1-\xi)^2} \frac{1}{(1-T)} \left[\frac{2}{T} \left(1 - \frac{\xi}{T} \right) - 1 + \left(\frac{\xi}{T} \right)^2 \right]; \quad [\text{A.2}]$$

and

$$\frac{d\xi}{dT} = \frac{\xi}{T} + \frac{1}{\lambda} \frac{1}{(1-T)} \frac{1}{(1-\xi)} \left(1 - \frac{\xi}{T} \right)^2. \quad [\text{A.3}]$$

Equations [A.1] and [A.3], with the initial condition $\xi = 0$ at $T = T_{in}$, describe both the shock and the outmost characteristic. As $\lambda \gg 1$, an approximation for this locus is sought, letting

$$\xi = \frac{1}{\lambda} \xi_1 + \frac{1}{\lambda^2} \xi_2 + \dots \quad [\text{A.4}]$$

From [A.3], the leading terms satisfy

$$\frac{d\xi_1}{dT} = \frac{\xi_1}{T} + \frac{1}{1-T}. \quad [\text{A.5}]$$

The solution, accounting for initial conditions, is

$$\xi_1 = T \ln \frac{T(1-T_{in})}{T_{in}(1-T)}$$

and, in view of [A.1], one obtains

$$\xi_1(T, Z) = T \ln \frac{1-TZ}{(1-T)Z}. \quad [\text{A.6}]$$

It is noted that the consistency of [A.5] requires $(\xi_1/T) \ll \lambda$, which is not too restrictive, since spin-up is of interest during $\tau \leq 2$ ($T \leq 0.98$). However, the midplane region $Z \rightarrow 0$ is problematic, as already pointed out.

In view of [A.4] and [A.6], [A.2] is approximated by

$$\frac{d\varepsilon}{\varepsilon} = \frac{1}{\lambda} \frac{1}{(1-T)} \frac{2}{T} + O\left(\frac{1}{\lambda^2}\right). \quad [\text{A.7}]$$

With $\varepsilon = \varepsilon(0)$ at T_{in} , and using [A.1], the integration of the leading term gives:

$$\ln \frac{\varepsilon}{\varepsilon(0)} = \frac{1}{\lambda} \ln \frac{T^2(1-T_{in})}{T_{in}^2(1-T)} = \frac{1}{\lambda} \ln \frac{1-TZ}{(1-T)Z^2}. \quad [\text{A.8}]$$

Comparisons between the numerical solution of [A.2] and [A.3] and approximations [A.6]–[A.8], for $\lambda = 20$ and 50 display good agreement. The approximations overestimate both ξ_1 and $\varepsilon/\varepsilon(0)$ and can therefore be used as bounds for these variables. This feature was anticipated, because it can be easily shown that the neglected terms on the r.h.s. of both [A.5] and [A.7] are negative.